Perturbed angular correlation spectroscopy applied to the spin-glass systems *Au*Fe and *Cu*Mn

M. Rots, L. Hermans, and J. Van Cauteren
Instituut voor Kern- en Stralingsfysika, Katholieke Universiteit Leuven, B-3030 Leuven, Belgium
(Received 13 December 1983; revised manuscript received 30 March 1984)

Perturbed angular correlation spectroscopy has been shown to be a simple and reliable technique, comparable to muon spin precession spectroscopy, in the study of the magnetic phase diagram in alloys such as $Au_{1-x}Fe_x$ and $Cu_{1-x}Mn_x$. The spin-glass freezing at T_g is found to be a cooperative process. The mean magnetic hyperfine field in the vicinity of the ^{111}Cd probe follows, below T_g, a universal $(1-T/T_g)^{\beta}$ correlation with $\beta \simeq 0.45$. For *Au*Fe below 16 at. % Fe, the hyperfine field depends linearly on the freezing temperature, while for *Cu*Mn a $(T_g)^{3/2}$ dependence is observed. At temperatures $T \leq 0.7T_g$ the magnetic hyperfine field is static with a broad distribution, while for $T \geq T_g$ the alloys are paramagnetic.

We report on the first attempt using perturbed angular correlation (PAC) spectroscopy to study the local magnetic field distribution associated with spin-glass ordering in alloys like *Au*Fe and *Cu*Mn. The magnetic phase diagram *Au*Fe (Ref. 1) is rather complicated below 20 at. % Fe. Four different phases were reported: spin glass below 10 at. %, cluster glass coexisting with apparent ferromagnetic ordering as well as a ferromagnetic region. Recent Mössbauer experiments[2,3] clearly indicated the coexistence of a ferromagnetic and cluster-glass phase in $Au_{82}Fe_{18}$ and also detected a magnetic double transition in the paramagnetic—ferromagnetic—spin-glass freezing. Although the latter results confirmed the result[4,5] from earlier ac-susceptibility measurements as well as theoretical predictions,[6] the nature of the ferromagnetism is not clear. On the basis of magnetization results Beck[7] concluded that despite the increasing ferromagnetic spin correlation, no long-range ferromagnetism is developed with increasing iron concentration. The small-angle neutron scattering results by Murani[8] were also interpreted as first-neighbor ferromagnetic spin correlation appearing at a critical temperature T_c, but persisting below a lower temperature T_g where the long-range Ruderman-Kittel-Kasuya-Yosida interaction creates the spin-glass ordering. In order to provide information from another technique, we present our perturbed angular correlation (PAC) results. These experiments can be done at any temperature with or without an external field and allow us to probe, on a microscopic scale, the spontaneous magnetization throughout the sample, thus deciding whether or not long-range ferromagnetism is present. Being in many aspects similar to muon spin precession (μSR) experiments, PAC is more widely applicable and therefore it may be of interest to investigate the possibilities of this technique. The potential usefulness of PAC was discussed already in a short note[9] on *Au*Fe results. Here we add new information obtained on the *Cu*Mn system and we discuss the sensitivity of PAC concerning the probability distribution function of the local magnetic hyerfine field.

The basic principle of PAC (Ref. 10) is the observation of the nuclear spin precession through the angular distribution of γ radiation. By measuring a first γ ray in a fixed direction a spatial correlation of the second γ-rays in a nuclear decay cascade is observed. This correlation is a consequence of the nuclear spin alignment in the intermediate nuclear state, determined by the first radiation. When the nuclear moment interacts with an extranuclear electromagnetic field the nuclear spin in the intermediate state precesses causing the correlation anistropy to change. Therefore, the coincidence probability between both γ radiations, measured at fixed angles, becomes time dependent. This time modulation shows up with a characteristic frequency determined by the interaction strength in those cases where the interaction is unique. In random magnetic systems, however, the interaction strength changes from site to site and a smeared-out precession will be observed.

The magnetization in our samples was probed by observing the hyperfine (hf) interaction during the 125-ns mean lifetime of the 247-keV nuclear state in ^{111}Cd. The 2.8-d halflife ^{111}In decays through electron capture to ^{111}Cd, feeding the 173—247 keV (γ-γ) cascade. Data acquisition with a four-detector system allows us to calculate

$$R(t)=\frac{W_{AC}(\pi,t)W_{BD}(\pi,t)}{W_{AD}(\pi/2,t)W_{BC}(\pi/2,t)}-1=3A_2G_2(t)\ , \quad (1)$$

where $W_{AC}(\pi,t)$ is the true coincidence in a small time interval (time resolution typically 2 ns) when the angle between the detectors is π radians. In Eq. (1) the correlation anisotropy A_2 is known from nuclear-physics parameters, while $G_2(t)$ contains the so-called perturbation factor[10] including the hyperfine interaction.

I. SAMPLE PREPARATION

The alloys were produced by melting the high-purity constituents in an induction furnace under a continuous flow of dried argon. Samples were prepared in the concentrations 6.4, 8.4, 14.7, and 18 at. % iron for the *Au*Fe alloy and 5, 8, and 17 at. % Mn for the *Cu*Mn alloy. The nominal concentrations were verified by microprobe

analysis. After melting, the alloys were rolled to obtain a foil on which the indium activity from a carrier-free solution was deposited and dried. Further sample processing was different for both types of alloys.

The radioactive *Au*Fe foils were melted in the induction furnace, again under argon atmosphere. In order to distribute the activity throughout, the sample was kept in a molten state for a few minutes and then rolled again to foil thicknesses of approximately 90 μm. Annealing for typically 3 h at 900 °C in a argon atmosphere was ended by quenching from the oven directly into liquid nitrogen. After storage at 77 K the surface of the foil was chemically cleaned before being mounted in the PAC setup. Some measurements, however, were done on samples heat treated in a slightly different way. The alloys 6.4 and 18 at. % Fe (sample A) were annealed at 900 °C for 1 h only. The second 18 at. % Fe sample (sample B) was annealed for 40 h at 900 °C, while the third (sample C) was given the identical thermal treatment of that of sample B, but the activity was, after quenching, introduced by ion implantation at room temperature to a dose of 10^{13} ions/cm^2 without further treatment. All samples were first measured at 300 K and then cooled by a variable temperature cryostat in the 4—300 K temperature region.

The radioactive In isotope was introduced into the matrix of the *Cu*Mn alloys by diffusion under H_2 atmosphere for $\frac{1}{2}$ h at 450 °C, immediately followed by thermal annealing for 1 and $\frac{1}{2}$ h at 900 °C. Subsequently the alloy was quenched in water and mounted in the cryostat to take the 300-K spectrum. Further measurements were done after cooling down to 4.2 K.

II. INTERPRETATION OF PAC SPECTRA

Some typical PAC spectra for the $Au_{82}Fe_{18}$ alloy at different temperatures are displayed in Fig. 1. The data collected at $T=300$ and 109 K can be fitted very well on the basis of an expression[10] including a pure static quadrupole interaction:

$$G_2^Q(t)=\sum_{n=0,3} a_n \exp(-\delta\omega_n t)\cos(\omega_n t)\ , \tag{2}$$

with ω_n and $\delta\omega_n$ the quadrupole-interaction frequencies and widths, respectively.

At 10 K, however, the data substantially deviate from such a curve, showing that another interaction suppresses the quadrupole response. A similar and even more drastic change in the PAC spectrum shape is illustrated in Fig. 2 for the $Cu_{95}Mn_5$ alloy at temperature $T=12$ and 20 K, the room-temperature spectrum being essentially the same as the one at 20 K. Clearly the alloys are in a paramagnetic state (pure quadrupole interaction) at room temperature and undergo a phase transition upon cooling, which we associate with the spin-glass freezing. Below a critical temperature a distribution in magnetic hyperfine fields at the nuclear probe is established. In order to reproduce the data at low temperature an analytical expression for $R(t)$ is needed, depending upon the particular distribution $P(H)$ chosen for the exchange fields. A currently used distribution[11] for the magnitude of the field

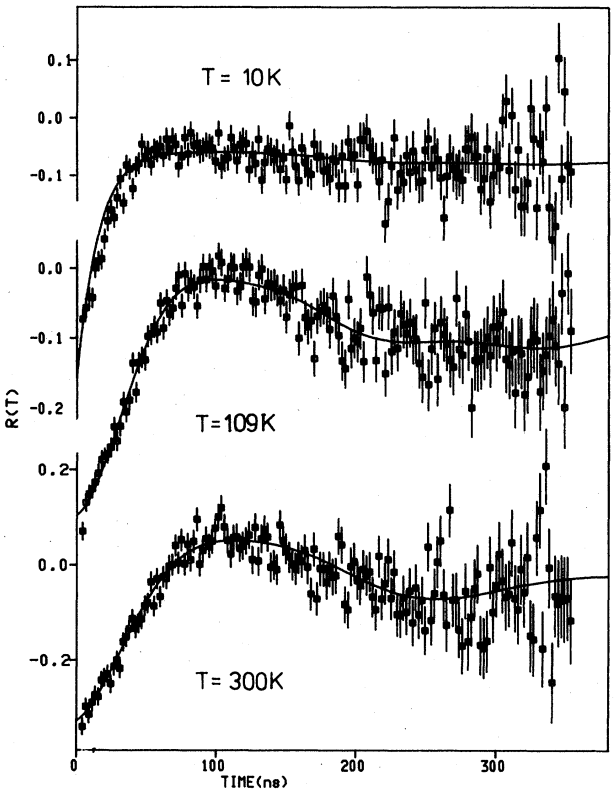

FIG. 1. Typical PAC spectra obtained with ^{111}In probe in $Au_{82}Fe_{18}$ alloy.

$$P(H)=\frac{4}{\pi}\frac{\Delta H^2}{(\Delta^2+H^2)^2} \tag{3}$$

was also inferred from computer simulations.[12] The corresponding $G_2(t)$ may be written as[9]

$$G_2(t)=\left[\frac{1}{5}+\frac{2}{5}\sum_{n=1,2}\exp(-n\Delta t)(1-n\Delta t)\right] \times\left[\sum_{n=1,3} a_n \exp(-\delta\omega_n t)\cos(\omega_n t)\right]\ . \tag{4}$$

The first part of this expression is very similar to the depolarization function derived for the μSR experi-

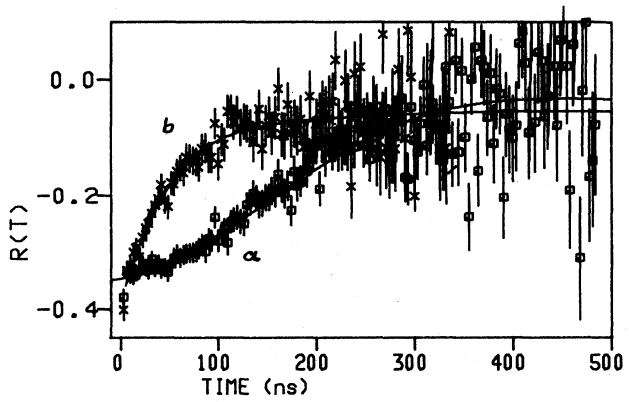

FIG. 2. PAC spectra for $Cu_{95}Mn_5$ at 20 K (a) and 12 K (b).

ments,[13,14] while the second part represents the electric quadrupole interaction.

With the parameter Δ having the meaning of a most probable field value the expression (4) may be interpreted as a depolarization of the nuclear alignment, the latter oscillating periodically under the influence of a static quadrupole interaction with strength ω_n. This electric quadrupole interaction results from the broken cubic lattice symmetry due to the randomly distributed magnetic impurities, and can be easily determined at 300 K where the alloys are paramagnetic and therefore $\Delta=0$.

Another choice of a static hyperfine field distribution may have a Gaussian or Lorentzian shape with nonzero mean value H_0 and width δH_0. Such a distribution combined with the quadrupole interaction of strength ω_0 and width $\delta\omega_0$ results in a perturbation factor:

$$G_2(t)=\tfrac{1}{5}+\tfrac{4}{35}\cos[(\gamma H_0+\omega_0)t]\exp[-(\gamma\delta H_0+\delta\omega_0)t]+\tfrac{10}{35}\cos[(\gamma H_0+2\omega_0)t]\exp[-(\gamma\delta H_0+2\delta\omega_0)t]$$
$$+\tfrac{9}{35}\cos[(2\gamma H_0+\omega_0)t]\exp[-(2\gamma\delta H_0+\delta\omega_0)t]+\tfrac{5}{35}\cos[(2\gamma H_0+3\omega_0)t]\exp[-(2\gamma\delta H_0+3\delta\omega_0)t]\ . \quad (5)$$

Once more ω_0 and $\delta\omega_0$ are determined at 300 K and the data at lower temperatures can be fitted with two free parameters H_0 and δH_0. If below the transition temperature the magnetic impurity spins are frozen in, the PAC probe will experience a static magnetic field. Then the expressions (4) or (5) should allow a good fit to the data, thereby supporting the frozen-spin hypothesis.

Angular distribution measurements of the type discussed here may also be sensitive to the effect of dynamical fluctuations of the Fe or Mn moments. In much the same way as extensively discussed by Hayano *et al.*[13] for zero-field μSR experiments, PAC spectroscopy can distinguish the static interaction case from dynamical modulation in those cases where the quadrupole interaction is small. While static perturbations lead to periodic functions $G_2(t)$ of the type Eq. (5) in the limit of fast fluctuations, time-dependent hyperfine interaction fluctuations produce just an exponential relaxation,

$$G_2(t)=\exp(-\lambda_2 t)\ . \quad (6)$$

When the correlation time is short the magnetic interaction averages to zero and the nuclear probe senses a static quadrupole interaction (paramagnetic case). At the transition temperature where the magnetic moments on the impurities become locked in random directions the relaxation curves depend upon the ratio of the fluctuation rate over the average hf field $\langle H_i\rangle$.[14] Then the perturbation factor $G_2(t)$ is rather complex and an analytical expression can be derived only in special cases.[15] As the spin-glass state is established by a gradual slowing down of spin fluctuations we may expect to observe a transition when the correlation time is within the (10^{-7}–10^{-8} s) time window of our experiment. A fairly abrupt changeover from a paramagnetic PAC spectrum without hyperfine field toward a static hyperfine field spectrum should then be observable around the spin-glass transition temperature. A distribution in blocking temperatures may then be reflected in the PAC data through a nonunique site response, i.e., some of the probes experience a pure quadrupole interaction [Eq. (2)] simultaneously with another fraction experiencing a combined static magnetic plus electric interaction [Eqs. (4) or (5)].

III. RESULTS

The raw data in our PAC experiments consists of four time spectra containing the coincidence probability $W(\theta,t)$ as a function of time t measured at a fixed angle θ between the radiation directions. As given by Eq. (1) the spin precession function $R(t)$ was calculated and the resulting data were fitted using Eqs. (4) or (5). In this fitting procedure we searched for the temperature below which the room-temperature fit function [Eq. (2)] was no longer satisfactory. The only assumption made was that

TABLE I. Parameters in the temperature behavior [Eq. (7)] of the hyperfine field.

c (at.%)	B(kG) ($T=0$ K)	T_g (K)	β	Quadrupole interaction (Mrad/s) ω_Q	$\delta\omega_Q$
*Au*Fe					
6.4	11.7(2)	28(1)	1.32(3)	1.47(7)	0.39(15)
8.4	13.8(5)	35(2)	0.51(4)	3.5(1)	0.36(10)
14.7	17.5(3)	51(1)	0.44(2)	3.3(1)	0.9(2)
18.0(*A*)	13.6(8)	67(1)	1.08(10)	4.0(1)	0.3(1)
18.0(*B*)	17.9(7)	50(1)	0.45(6)	2.9(1)	0.57(6)
18.0(*C*)	26.8(9)	60(1)	0.57(3)	2.8(1)	1.1(1)
*Cu*Mn					
5.0	3.8(3)	15(1)	0.35(10)	0.60(2)	0.14(5)
8.0	14.1(2)	35(1)	0.45(1)	1.1(1)	0.25(3)
17.0	30.8(2.3)	60(1)	0.45(5)	1.8(1)	0.70(4)

as soon as a magnetic hyperfine field shows up, the quadrupole interaction, always present, is smaller than any magnetic interaction experienced by the probe nuclei. This approximation is valid for temperatures not too close to the transition temperature.

The data on *Au*Fe alloys were analyzed on the basis of Eq. (4) and the mean field value $\Delta=\gamma B$ ($\gamma=1.46$ kHz/G) was determined as a function of temperature. For each concentration the $\Delta(T)$ values were fitted with the expression

$$B(T)=B_0(1-T/T_g)^{\beta} \tag{7}$$

using three free parameters, B_0, T_g, and β. In Table I we list the results together with the quadrupole interaction parameters $\omega_Q=(eQV_{zz})/\hbar 4I(2I-1)$ and $\delta\omega_Q$.

As can be seen from this table the three experiments on the 18 at. % *Au*Fe alloy differ in all three fit parameters. In Fig. 3 we collect all $B(T)$ data, except 6.4 and 18 at. % *A* and *C*, in reduced scales $B(T)/B_0$ and T/T_g. A reasonable fit to all of the data using Eq. (7) yields $\beta=0.46(1)$, showing that the freezing mechanism is similar for all measured concentrations. Using this β value the concentration dependence of B_0 as well as T_g was compared to a C^{γ} behavior yielding

$$B_0(C)=5.3(3)C^{0.44(3)}\ (\text{kG})\ ,$$

$$T_g(C)=8.6(2)C^{0.66(1)}\ (\text{K})$$

with C in at. % Fe concentration. From a compilation by Larsen[16] the freezing temperature T_g taken from Mössbauer and susceptibility work depends on concentration according to $9.5(2)C^{0.58(1)}$ and $7.9(2)C^{0.63(1)}$, respectively, in good agreement with our result for this limited data set.

For the *Cu*Mn alloy, noticing that the quadrupole interaction is much smaller, a similar analysis as detailed above was based on Eqs. (4) and (5). The PAC spectra for all temperatures, shown in Fig. 4 for the $Cu_{92}Mn_8$ alloy, were fitted with the two alternative functions but are much better reproduced by the function Eq. (5), i.e., a static nonzero magnetic interaction with a broad distribution. A similar misfit was also noticed in the *Au*Fe spec-

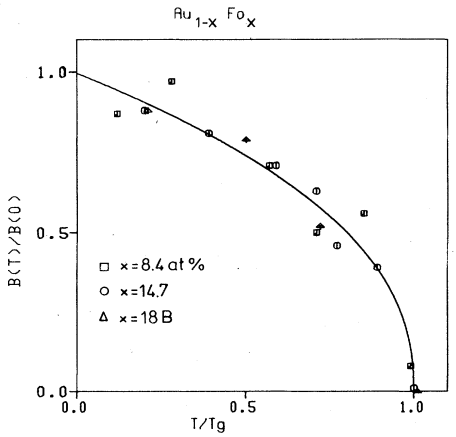

FIG. 3. Universal behavior of the reduced mean hyperfine field in the spin-glass regime for *Au*Fe according to Eq. (7).

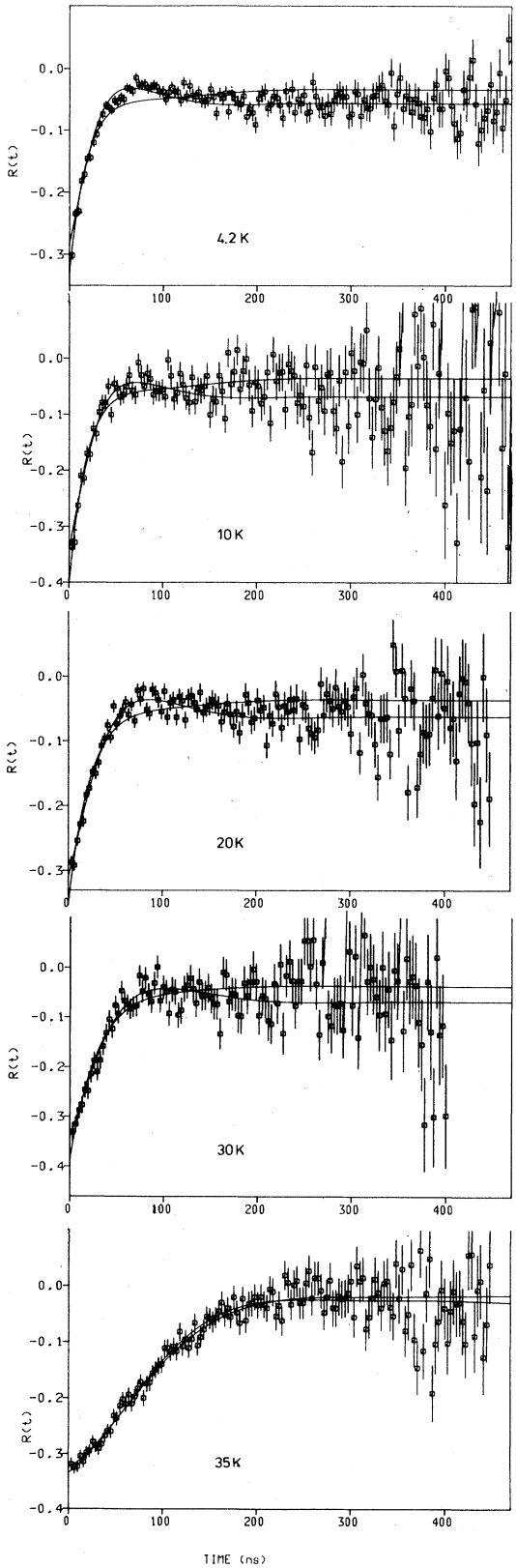

FIG. 4. Least-squares-fit results for two $P(H)$ distributions in $Cu_{92}Mn_8$ using Eqs. (4) and (5).

tra at lower temperatures, but obscured by the stronger and nonaxially symmetric quadrupole interaction. The temperature dependence of the mean local field in *Cu*Mn is the same for both fit functions and is displayed in Fig. 5(a). The temperature behavior of the relative interaction width $\delta H_0/H_0$ is plotted for the $Cu_{92}Mn_8$ in Fig. 5(b), showing a steep increase close to the transition temperature. This observation is indicative for the detection of dynamical relaxation processes in a narrow region at T_g. For all measured concentrations the *Cu*Mn mean hyperfine field at the Cd probe has a similar temperature behavior, as shown in Fig. 6. The solid lines correspond to the function Eq. (7) and the parameters are given in Table I. It is interesting to note that essentially the same value for β is found for both alloy types. The transition temperatures T_g observed in these experiments are in good agreement with existing data[17] for both alloy types. Moreover, a correlation between the extrapolated hf field (B_0) and the transition temperature T_g is established. While *Au*Fe shows, below 16 at.% Fe, a linear relation B_0 versus T_g, *Cu*Mn alloys are better reproduced taking B_0 proportional to $(T_g)^{3/2}$. It should be noted that this correlation in *Au*Fe breaks down at 18 at.% Fe, where the magnitude of the hyperfine field as well as T_g stabilize near the 15 at.% value. Probably this may indicate a change in randomness of the alloy due to increasing atomic clustering during quenching. Extension of PAC measurements to higher-concentration alloys may be valuable.

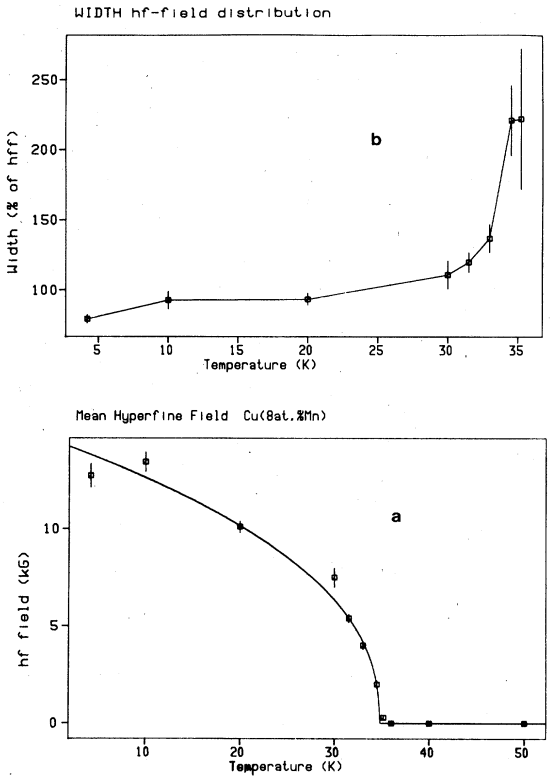

FIG. 5. Temperature dependence of the mean hyperfine field (a) and interaction width (percent of mean value) (b) for the $Cu_{92}Mn_8$ alloy.

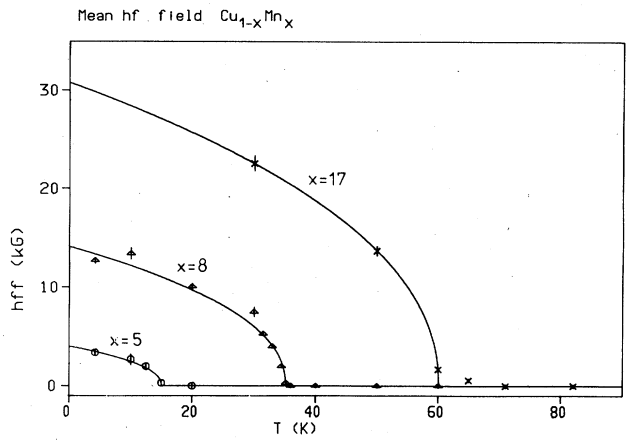

FIG. 6. Temperature dependence of the mean hyperfine field for $Cu_{1-x}Mn_x$ alloys.

IV. DISCUSSION

From the above results we may conclude that PAC on a nuclear probe can observe the spin-glass freezing process in zero external field quite well. The temperature dependence of the PAC spectra on $Cu_{95}Mn_5$ at 12 and 20 K (Fig. 2) is an illustration of the sensitivity (see also Fig. 4). From the discussion on the experimental conditions it should be clear that present technique compares very well with μSR and similar information may be derived. Due to the probe (with a rather large quadrupole moment) chosen here, our experiment is the analog of transverse field μSR, the role of the external field taken over by the electric quadrupole interaction. Here also discrimination between static and dynamic effects is limited, but in this case by the quadrupole-interaction strength ω_Q. We anticipate, that by choosing a probe with a smaller quadrupole moment much more sensitivity regarding the distribution can be attained. In this case we approach the zero-field condition of μSR and more detailed information on the relaxation function may be derived. This expected improvement is already indicated by the *Cu*Mn results. Here the quadrupole interaction is roughly a factor of 3 smaller than in *Au*Fe and Fig. 4 demonstrates more sensitivity regarding the $P(H)$ distribution.

The temperature dependence of the local field $B(T)$ (Figs. 3 and 6) is found to be the same for both alloy types and universal in respect to the magnetic impurity concentration, but the concentration dependence of the mean-field value extrapolated to zero temperature (B_0) is not linear, as should be expected theoretically.[11] The local field we measured is related to the Edwards-Anderson order parameter $[q(T)]^{1/2}$, which is theoretically proportional to $(T_g - T)^{1/2}$ in the infinite-range model.[6] Here we find a critical exponent $\beta \simeq 0.45$ for *Au*Fe as well as *Cu*Mn down to the lowest temperatures.

In the neutron scattering experiment of Murani and Heidemann,[18] the systematic differences between T_g temperatures derived from Mössbauer and susceptibility techniques was explained in terms of a wide spectrum in relaxation rates. Our PAC transition temperatures are in good agreement with existing data[17] for both *Au*Fe or

*Cu*Mn, except at the higher concentrations in *Au*Fe. Our values are substantially lower for the $Au_{82}Fe_{18}$ alloy. This discrepancy is not related to a different time window, which for the present probe is comparable with the Mössbauer experiment.

We observed changes in T_g for the 18 at. % *Au*Fe samples depending upon the sample preparation. It is known[19] that differing thermal annealing or radiation damage affect the actual spatial magnetic impurity distribution. Moreover, we observe a quadrupole interaction in *Au*Fe which is almost concentration independent (Table I). This, in combination with a repulsive Fe-In interaction in gold,[20] may indicate chemical iron clustering at relatively large distances from our probe. The double magnetic transition claimed in Mössbauer polarization experiments[2] as well as susceptibility data[4] is not observed here, although our $T_g = 50$—60 K matches with the temperature where the second transition should take place upon cooling. As seen by the cadmium probe, the $Au_{82}Fe_{18}$ alloy transforms from the paramagnetic state directly into the spin-glass state. This statement is not dependent on any prejudice in the data analysis, but stems simply[21] from the fact that the room-temperature PAC spectrum remains unchanged down to 60 K. This apparent disagreement may probably be explained from the fact that our In probe is located preferentially in the matrix instead of in the magnetic clusters present[1] in *Au*Fe alloys of concentration above 10 at. % Fe. The recent interpretation[22] of Mössbauer results on *Au*Fe, in terms of two distinct compositional "phases," may probably be linked with our PAC results in $Au_{82}Fe_{18}$ and the observed breakdown of the linear B_0 versus T_g correlation. Furthermore, it may be interesting to note that in both *Au*Fe and *Cu*Mn alloys the temperature dependence of the hyperfine field results in nearly the same critical exponent $\beta \simeq 0.45$. This is more remarkable in view of the expectation[23] that the clusters in *Au*Fe freeze much more gradually than do those in the *Cu*Mn matrix with predominantly antiferromagnetic spin correlation.

As a final remark we point out that the PAC results can be very well reproduced assuming that all probes behave collectively around the transition temperature, all of them sensing the same interaction simultaneously. Especially from the *Cu*Mn data [Fig. 5(b)] it is clear that all probes at $T < 0.7T_g$ experience a static magnetic interaction with a nonzero mean value but with a broad distribution (90% of the mean field). This cooperative behavior suggests a phase transition as predicted in the Edwards-Anderson hypothesis of frozen-in and randomly oriented spins of the paramagnetic impurity centers. A gradual freezing with a distribution of blocking temperatures seems to be excluded from the fact that the data are very well reproduced by assuming a probe environment characterized by a broad but a single hyperfine-field distribution. In the present experiments the probe becomes aware of a hyperfine field at a temperature where the thermal reorientation of "cluster" moments is slower than roughly 10^{-8} s. From a broad distribution in blocking temperatures we may expect, contrary to our observation, a complex PAC spectrum around T_g. Nevertheless, we refrain from deciding between these models in view of the present initial stage of PAC work in this area.

ACKNOWLEGMENTS

The authors are very much indebted to Professor P. A. Beck for his stimulating interest and relevant comments. Also, the help of Dr. O. Arkens (Department of Metaalkunde en Toegepaste Materiaalkunde, Katholieke Universiteit Leuven) is gratefully acknowledged. This work was financially supported by the Belgian Universitair Instituut voor Kernwetenschappen.

[1] B. V. B. Sarkissian, J. Phys. F **11**, 2191 (1981).
[2] J. Lauer and W. Keune, Phys. Rev. Lett. **48**, 1850 (1982).
[3] I. A. Campbell, S. Senoussi, F. Varret, J. Teillet, and A. Hamzic, Phys. Rev. Lett. **50**, 1615 (1983).
[4] B. H. Verbeek and J. A. Mydosh, J. Phys. F **8**, L109 (1978).
[5] B. H. Verbeek, G. J. Nieuwenhuys, H. Stocker, and J. A. Mydosh, Phys. Rev. Lett. **40**, 586 (1978).
[6] S. Kirkpatrick and D. Sherrington, Phys. Rev. B **17**, 4384 (1978).
[7] P. A. Beck, Solid State Commun. **34**, 581 (1980).
[8] A. P. Murani, Solid State Commun. **34**, 705 (1980).
[9] M. Rots, J. Van Cauteren, and L. Hermans, J. Appl. Phys. **55**, 1732 (1984).
[10] W. Witthuhn and W. Engel, in *Topics in Currrent Physics,* edited by J. Christiansen (Springer, New York, 1983), Vol. 31, p. 205; E. Recknagel, in *Site Characterization and Segregation of Implanted Atoms in Metals,* edited by A. Perez and R. Coussement (Plenum, New York, 1978), p. 223.
[11] M. W. Klein, L. J. Schowalter, and P. Shukla, Phys. Rev. B **19**, 1492 (1979).
[12] L. R. Walker and R. E. Walstedt, Phys. Rev. B **22**, 3816 (1980).
[13] R. S. Hayano, Y. S. Uemura, J. Imazato, N. Nishida, T. Yamazaki, and R. Kubo, Phys. Rev. B **20**, 850 (1979).
[14] A. F. Fiory, Hyp. Interact. 8, 777 (1981).
[15] J. Bosse, H. Gabriel, and W. Vollmann, Hyp. Interact. **1**, 33, (1975).
[16] U. Larsen, Phys. Rev. B **18**, 5014 (1978).
[17] P. A. Beck, Prog. Mater. Sci. **23**, 1 (1978).
[18] A. P. Murani and A. Heidemann, Phys. Rev. Lett. **41**, 1402 (1978).
[19] R. J. Borg, D. Y. F. Lai, and C. E. Violet, Phys. Rev. B **5**, 1035 (1972).
[20] A. R. Miedema, F. R. de Boer, and R. Boom, Calphad **1**, 341 (1977); K. Krolas, Phys. Lett **85A**, 107 (1981).
[21] M. Rots, L. Hermans, and J. Van Cauteren, Solid State Commun. **49**, 131 (1983).
[22] C. E. Violet and R. J. Borg, Phys. Rev. Lett. **51**, 1073 (1983).
[23] P. A. Beck, Phys. Rev. B **23**, 2290 (1981).